

Production of innovative radionuclides for therapy and diagnostics: nuclear data measurements and comparisons with TALYS code

A. Guertin¹, E. Nigron¹, M. Sitarz^{2,3}, C. Duchemin^{1}, F. Haddad^{1,2}, V. Métivier¹*

¹ Subatech laboratory, CNRS/IN2P3, IMT Atlantique, Université de Nantes, Nantes, France

² GIP ARRONAX, Saint-Herblain, France

³ University of Warsaw, Warszawa, Poland

* now at CERN, HSE-RP group, Geneva, Switzerland

Abstract

Nuclear medicine is a specialty that uses radioactive nuclei for therapy or diagnostic of diseases such as different types of cancer. The aim of this paper is to give the status of nuclear data collected for medical isotopes production and to present the large set of experimental data collected by the PRISMA team of the Subatech laboratory using the protons, deuterons and alpha particles delivered by the ARRONAX cyclotron from few MeV up to 70 MeV and covering a wide range of target masses. Using these data, we will also show that constraints can be put on simulation tools such as the TALYS code (version 1.9) and compare with TENDL-2015, the TALYS-based evaluated nuclear data library. A better overall agreement with our experimental data could be obtained with a different combination of models already included in the code.

1 Introduction

Our research activities are focused on radionuclide production mainly for medical applications, either for therapy or diagnosis. This work is carried out in close collaboration with the GIP ARRONAX that possesses a high energy and high intensity multi-particle cyclotron [1]. In this frame, production cross sections and thick target yields were measured for alpha emitters, such as the U-230/Th-226, Th-227/Ra-223 and Ac-225/Bi-213 generators [2]; for photon, Tc-99m [2], and positon, Sc-44g [3], emitters for diagnosis; for electron emitters Re-186g [4], Tb-155 [5] and Sn-117m [6] for therapeutic applications. From the irradiated materials, new experimental production cross section data of interest for medical applications and monitor reactions have been extracted which allow to expand our knowledge on these excitation functions, to confirm the existing trends and to give additional values on a wider energy range. These experiments were conducted at the ARRONAX facility using the stacked-foil technique.

This data set only represents a small part of the data needed in the field studying the production of innovative radionuclides for medical applications. In order to get answers quickly without the need of new experiments, it is interesting to use theoretical models. The TALYS code gather together several of such models for each step of a nuclear interaction. A systematic comparison of our results with the output of the TENDL-2015 nuclear data library and TALYS code (version 1.9) has been done. In this latter case, several combinations of models have been tested in order to better reproduce the available data.

2 Experimental set-up and production cross section calculation

The production cross section data are obtained using the stacked-foil method [2, 7], which consists of the irradiation of a set of thin foils, grouped as patterns. Each pattern contains a target to produce the

isotopes of interest. Each target is followed by a monitor foil to have information on the beam intensity thanks to the use of a reference reaction recommended by the International Atomic Energy Agency [8]. A degrader foil is placed after each monitor foil to change the incident beam energy from one target foil to the next one. Each foil in the stack is weighed before irradiation using an accurate scale ($\pm 10\text{-}5$ g) and scanned to precisely determine its area. The thickness is deduced from these values, assuming that it is homogeneous over the whole surface. In this work, we used thin target and monitor foils of a few tens of micrometres thick and degrader foils of few hundreds of micrometres thick. All foils were purchased from the Good Fellow[©] company.

These foils were irradiated by proton (up to 70 MeV), deuteron (up to 34 MeV) or alpha particle (68 MeV) beams provided by the ARRONAX cyclotron. It delivers these beams with an energy uncertainty of ± 0.50 MeV, ± 0.25 MeV and ± 0.61 MeV, respectively for p, d or alpha particle, as specified by the cyclotron provider using simulations. The beam line is under vacuum and closed using a 75 μm thick kapton foil. The stacks were located about 6.8 cm downstream in air. The energy through each foil has been determined in the middle of the thickness of the foil using the SRIM software [9]. Energy losses in the kapton foil and air have been taken into account in our analysis. All along the stack, depending on the number of foils, the energy uncertainty increases up to ± 2.0 MeV due to the energy straggling. Irradiations were usually carried out for half an hour, with beams of mean intensity between 100 and 150 nA for proton, between 50 and 140 nA for deuteron and between 140 and 200 nA particles for alpha beam. The recommended production cross section values [8] of the Ti-nat(d, x)V-48 (all energies), Cu-nat(p,x)Co-56, Zn-62 (> 50 MeV), Ti-nat(p,x)V-48 (< 20 MeV), Ni-nat(p,x)Ni-57 (20-50 MeV), Cu-nat(α ,x)Ga-67 (up to 50 MeV) and Al-27(α ,x)Na-22 (from 50 MeV to 70 MeV) reactions were used to get information on the beam intensity, depending on the investigated energy range.

The activity measurements in each foil were performed using a high purity germanium detector from Canberra (France) with low-background lead and copper shielding. The first measurements started the day after the irradiation (after a minimum of 15 hours cooling time) during one hour, for all target and monitor foils. Our data are then limited to γ emitter radionuclides with a half-life higher than few hours. A second series of measurements was performed one week after End Of Beam, during a minimum of 24 hours (one day) and up to 60 hours. Third measurements were devoted to long half-life radionuclides and also waiting for the decay of some radionuclides. Gamma spectra were recorded in a suitable geometry calibrated in energy and efficiency with standard Co-57, Co-60 and Eu-152 gamma sources from LEA-CERCA (France). The full widths at half maxima were 1.04 keV at 122 keV (Co-57 γ ray) and 1.97 keV at 1332 keV (Co-60 γ ray). The samples were placed at a distance of 19 cm from the detector, which is suited to reduce the dead time and the effect of sum peaks. The dead time during the counting was always kept below 10%.

The production cross section values are calculated using the well-known activation formula, defined as a relative equation in which the knowledge of the beam current is no longer necessary thanks to the recommended reactions. The uncertainty is expressed as a propagation error calculation (see [6] for more details).

3 The TALYS code and TENDL data library

In this article, all the experimental production cross section values are compared with the version 1.9 of the TALYS code released in December, 2017 [10]. TALYS is a nuclear reaction program which simulates reactions induced by light particles, neutrons, photons, protons, deuterons, tritons, ^3He - and alpha-particles, on target nuclides of mass 12 and heavier. It incorporates theoretical models to predict observables including production cross section values as a function of the incident particle energy (up to 1 GeV). A combination of models that best describes the whole set of available data for all projectiles, targets and incident energies have been defined by the authors and put as default in the

code. In this way, a calculation can be performed with minimum information in the input file: the type of projectile and its incident energy, the target type and its mass. The results of this combination of models are referenced in Fig. 1 to 4 as TALYS 1.9 Default.

TENDL is a TALYS-based Evaluated Nuclear Data Library using both default and adjusted TALYS calculations and data from other sources [10, 11]. Our experimental production cross section values have been compared with the 8th TENDL release: TENDL-2015. It provides evaluated data for seven types of incident particles (n, p, d, t, He-3, alpha-particle, gamma) and for all the isotopes living more than 1 second (~ 2800 isotopes), up to 200 MeV. Since there are some differences between experimental data and the results of the TALYS code using default models and the TENDL-2015 library, we have defined a combination of models, already included in the TALYS code, which better describes the production cross sections, for a variety of projectiles, incident energies and target masses. The description of the optical, pre-equilibrium and level density models have been found to have a great influence on the calculated production cross section values. When proton, deuteron and alpha particle are used as projectile, better results are in general obtained using the optical model described, respectively by [12], [13] and [14]. And for these three projectiles, when a pre-equilibrium model based on the exciton model including numerical transition rates with optical model for collision probabilities [15, 16] and a model for the microscopic level density from Hilaire's combinatorial tables [17] is used. The results of this combination of models are plotted in Fig. 1 to 4 as TALYS 1.9 Adj. Parametrizations of the models have not been changed. They are used as they are implemented in TALYS. Level density or optical model parameters haven't been tuned.

4 Results and discussion

TALYS version 1.9 results have been obtained using the default models (labelled Default) and using the combination of models (labelled Adj.) described in the section 3. In Fig. 1 to 4, the full circles correspond to our experimental values, the other geometrical symbols to literature data, the full lines to TALYS Default and the dash lines to TALYS Adj. calculations. Four reactions, extracted from previous published articles, are presented. They cover proton, deuteron, alpha particle beams and a wide range of masses. All the experimental production cross section values are compared with the version 1.9 of the TALYS code released in December, 2017 [10].

4.1 Th-226 production from the Th-232(p,3n)Pa-230 reaction

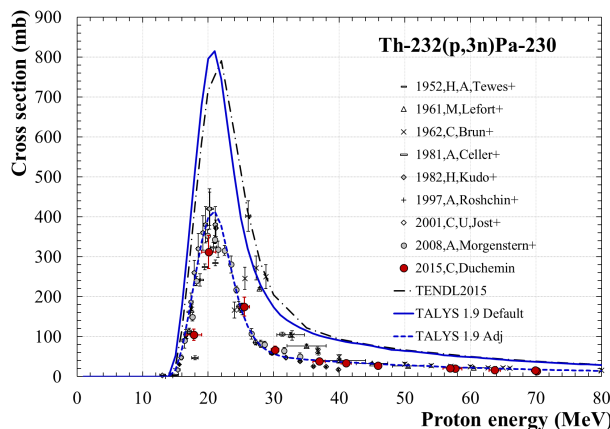


Fig. 1: Th-232(p,3n)Pa-230 cross section

Th-226 is a promising radionuclide for α RIT in leukaemia treatment. Th-226, with a half-life of 31 minutes, can be produced from the α decay of U-230, which has a half-life of 21 days, thanks to a

generator system U-230/Th-226. We studied the U-230 production using the Th-232(p,3n)Pa-230(β -)U-230 reaction. Our set of data for the Th-232(p,3n)Pa-230 reaction is plotted in Fig. 1.

There is a good agreement with our experimental data and those available in the literature. The TALYS code version 1.9 with default models and the TENDL-2015 library values, plotted with a dashed-pointed line, are not able to reproduce the production cross section amplitude even if the shape is in good agreement with our experimental data. The TALYS 1.9 Adj. results are in perfect agreement with these experimental data. As TENDL-2015 and TALYS 1.9 Default curves exhibit roughly the same shape and amplitude, TENDL-2015 will not be plotted on the following figures.

4.2 Re-186g production from natural tungsten

Re-186g, with a half-life of 3.7 days, is a β - emitter used in clinical trials for the palliation of painful bone metastases resulting from prostate and breast cancer. It emits a 137 keV gamma ray, suited for SPECT imaging. The Fig. 2 shows that our experimental production cross section values are in agreement with the literature. The TALYS 1.9 Default calculation is far from the cross section amplitude. The TALYS 1.9 Adj. values are in better agreement but still underestimate the maximum of the cross section by 20%.

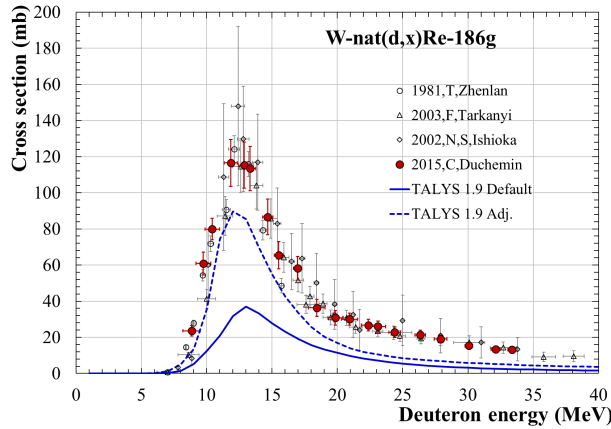


Fig. 2: W-nat(d,x)Re-186g cross section

4.3 Sn-117m production from natural cadmium

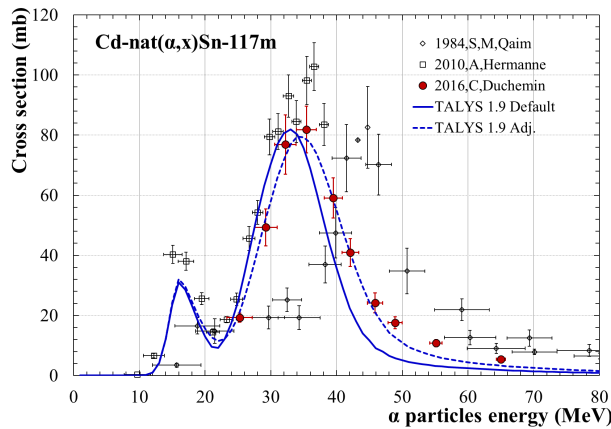


Fig. 3: Cd-nat(α ,x)Sn-117m cross section

Sn-117m is a conversion and Auger electron emitter, with a half-life of 13.6 days, useful for the palliation of painful bone metastases. Moreover, imaging can be achieved with its 158 keV gamma line. Our experimental production cross section values are in agreement with the values of Hermanne et al., published in 2010 (see Fig. 3). However, the Qaim and Döhler values show a shift in energy, roughly 10 MeV higher, for the location of the cross section's maximum. The points have been degraded rather far from the initial beam energy, which could explain the shift by energy straggling through the foils.

The TALYS 1.9 Default models give the good shape but results are slightly underestimated and shifted in energy (3 MeV lower). TALYS 1.9 Adj. models are in good agreement with the general behaviour of the experimental data. This combination allows reproducing the shape, the position of the maximum and the amplitude below 45 MeV.

4.4 Tb-115 production from natural gadolinium

Several terbium isotopes are suited for diagnosis or therapy in nuclear medicine. Tb-155 is of interest for SPECT imaging and/or Auger therapy. Tb-155 has a half-life of 5.32 days. It decays by electron capture process to Gd-155 (stable) by emitting Auger electrons (4.84 keV and 34.9 keV), conversion electrons (from 2 keV to 130 keV) and nine main gamma rays (from 86 keV to 367 keV).

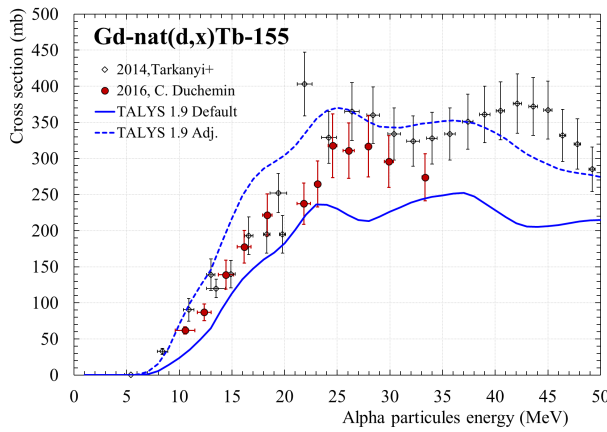


Fig. 4: Gd-nat(d,x)Tb-155 cross section

Our experimental production cross section values are plotted in Fig. 4. They are in agreement with the literature data set. The TALYS 1.9 Default models give the good shape but results are slightly underestimated. TALYS 1.9 Adj. models are in good agreement with the general behaviour of the experimental data but slightly overestimated the experimental results.

5 Conclusions

A large set of production cross section of medical radionuclides have been collected using the stacked-foil technique with proton, deuteron and alpha beams delivered by the ARRONAX cyclotron and for various materials on a wide range of masses. Some comparisons have been systematically performed with the TALYS code, version 1.9. This code has been chosen because it includes a large number of theoretical models, the possibility to combine these models to better describe the experimental data and because the authors' team is very reactive and helpful. Three main mechanisms have been investigated, which have a great impact on the studied observables in our work. They are the optical potential, the level density description and the pre-equilibrium model. A set of models have been found allowing a good description of all our collected data, which is different from the suggested

default combination of models. They can be used to get high quality data when no data are available in databases.

Acknowledgement

The ARRONAX cyclotron is a project promoted by the Regional Council of Pays de la Loire financed by local authorities, the French government and the European Union. This work has been, in part, supported by a grant from the French National Agency for Research called “Investissements d’Avenir”, Equipex Arronax-Plus No. ANR-11-EQPX-0004 and Labex No. ANR- 11-LABX-0018-01.

References

- [1] F. Haddad, L. Ferrer, A. Guertin, T. Carlier, N. Michel, J. Barbet, J-F. Chatal, Eur. J. Nucl. Med. Mol. Imaging 35, 1377–1387 (2008).
- [2] C. Duchemin, A. Guertin, F. Haddad, N. Michel, V. Métivier, Phys. Med. Biol. 60, 931-946 (2015).
- [3] C. Duchemin, A. Guertin, F. Haddad, N. Michel, V. Métivier, Phys. Med. Biol. 60, 6847-6864 (2015).
- [4] C. Duchemin, A. Guertin, F. Haddad, N. Michel, V. Métivier, Appl. Radiat. Isot. 97, 52-58 (2015).
- [5] C. Duchemin, A. Guertin, F. Haddad, N. Michel, V. Métivier, Appl. Radiat. Isot. 118, 281–289 (2016).
- [6] C. Duchemin, A. Guertin, F. Haddad, N. Michel, V. Métivier, Appl. Radiat. Isot. 115, 113-124 (2016).
- [7] G. Blessing, W. Brautigam, H.G. Boge, N. Gad, B. Scholten, S.M. Qaim, Appl. Radiat. Isot. 955, 46–49 (1995).
- [8] F. Tárkányi, S. Takács, K. Gul, A. Hermanne, M.G. Mustafa, M. Nortier, P. Oblozinsky, S.M. Qaim, B. Scholten, Yu.N. Shubin, Z. Youxiang, IAEA-TECDOC 1211, 49–152 (2001). Database available on https://www-nds.iaea.org/medical/monitor_reactions.html, updated Aug. 2017.
- [9] J.F. Ziegler, M.D. Ziegler, J.P. Biersack, Nucl. Instrum. Methods Phys. Res. B 268, 1818–1823 (2010).
- [10] A.J. Koning, D. Rochman, Nucl. Data Sheets 113 2841 (2012).
- [11] A.J. Koning, D. Rochman, J. Kopecky, J. Ch. Sublet, E. Bauge, S. Hilaire, P. Romain, B. Morillon, H. Duarte, S. van der Marck, S. Pomp, H. Sjostrand, R. Forrest, H. Henriksson, O. Cabellos, S. Goriely, J. Leppanen, H. Leeb, A. Plompen and R. Mills, https://tendl.web.psi.ch/tendl_2015/tendl2015.html.
- [12] A.J. Koning, J.P. Delaroche, Nucl. Phys. A 713 231 (2003).
- [13] Y. Han, Y. Shi, Q. Shen, Phys. Review C 73 (2006).
- [14] P. Demetriou, C. Grama, S. Goriely, Nucl. Phys. A 707 (1-2) 253-276 (2002).
- [15] E. Gadioli, P.E. Hodgson, Oxford Univ. Press (1992).
- [16] A.J. Koning and M.C. Duijvestijn, Nucl. Phys. A744 15 (2004).
- [17] S. Goriely, S. Hilaire, A.J. Koning, Phys. Review C 78 (2008).